www.czasopisma.pan.pl PAN POLSKA AKADEMIA NAUK www.journals.pan.pl

Arch. Metall. Mater. **68** (2023), 4, 1439-1446

DOI: https://doi.org/10.24425/amm.2023.146210

M.N. BABA[1*], G.D. VOINEA[2], M.E. LUCACI[3]

THREE-POINT BENDING RESPONSE OF NYLON 12 OBTAINED BY FUSED FILAMENT FABRICATION (FFF) VERSUS SELECTIVE LASER SINTERING (SLS)

This study analyses the three-point bending behavior of Nylon 12 (PA12) specimens produced using two additive manufacturing technologies (i.e., fused filament fabrication and selective laser sintering). A Nylon 12 commercially available filament (from Fiberlab S.A.) was selected to employ the fused filament fabrication method (FFF) with a Prusa 3D desktop printer, whereas Nylon 12 sintering powder (from Formlabs Inc.) was chosen for selective laser sintering (SLS) using a benchtop industrial SLS platform, Formlabs Fuse 1, with a powder refresh ratio of 30%. The bending strength and flexural elasticity moduli were determined by following ISO 178:2019 standard specifications to assess the effect of two different technologies on the mechanical behavior of three-point bending specimens produced in three distinct build orientations (i.e., 0°, 45°, and 90°) relative to the printing platform. One-way ANOVA analysis, Tukey's HSD, and Games-Howell tests are considered to assess the statistical variability of experimental data and compare the mean values of bending strength and flexural moduli. The testing results for the three orientations under question show notable differences and interesting similarities either in terms of strength or elasticity response for a significance *p*-level of 0.05.

Keywords: three-point bending; bending strength; flexural modulus; Nylon 12; Fused Filament Fabrication (FFF); Selective Laser Sintering (SLS)

1. Introduction

Over the last few years, 3D printed parts made with Nylon 12 have received widespread attention in various engineering and domestic applications due to their specific features that ensure sustainable conservation of the environment and its resources by an effective recycling system that keeps materials in use for as long as possible [1-4]. Within this context, selective laser sintering (SLS) has become the most popular additive manufacturing (AM) technology for Nylon 12. Since SLS typically uses laser energy as a heat source to locally melt and fuse the polymer powder particles, it can be used to produce relatively large parts with good mechanical properties and higher dimensional accuracy, especially compared with nozzle-based polymer deposition systems [5-7]. Besides, the freedom in the design of components and production, afforded by the nature of the SLS process, enables the effective handling of internally nested shapes without extra supporting structures and the possibility to print multiple parts within the same powder volume [8,9]. However, as SLS is a high-cost AM technology, its applicability, by a large, is justified for medium to high-scale engineering applications when lots of Nylon 12 parts with complex geometries, little anisotropy, and enhanced quality of external surfaces must be produced.

On the other hand, fused filament fabrication (FFF) uses the raw material in a filament form that is melted by a heater and then extruded through the nozzle in successive layers of beads against the printing platform. Although it sometimes involves a lot of trial and error pre-printing tests and often requires the use of support structures to prop up the parts during processing, FFF could represent a good compromise between processing costs, strength, stiffness, and toughness of printouts when creating prototypes with mid-fidelity requirements for small-scale production, domestic, or hobbyist applications.

At present, extensive research on the mechanical properties of FFF materials has been focused on polylactic acid (PLA) and acrylonitrile-butadiene-styrene copolymers (ABS) [10-14]. Nevertheless, these two materials perform unwell under corrosion conditions, high temperatures, wear, and fatigue, limiting their application in many engineering fields. Except for its high

[1] TRANSILVANIA UNIVERSITY OF BRAȘOV, DEPARTMENT OF MECHANICAL ENGINEERING, EROILOR BVD. 29, 500036, BRAȘOV, ROMANIA.
[2] TANSILVANIA UNIVERSITY OF BRAȘOV, DEPARTMENT OF AUTOMOTIVE AND TRANSPORT ENGINEERING, EROILOR BVD. 29, 500036, BRAȘOV, ROMANIA.
[3] ÉCOLE CENTRALE DE MARSEILLE, 38 RUE FRÉDÉRIC JOLIOT CURIE, 13013, MARSEILLE, FRANCE

* Corresponding author: mariusbaba@unitbv.ro

hygroscopicity, Nylon 12, also known by its chemical name Polyamide 12 (PA12), generally prevail over these drawbacks. However, its strength, stiffness, and toughness have been mainly investigated for SLS forms in terms of processing parameters [15-20], build orientation, and anisotropy [21-28], optimization, morphology, and multiscale characterization [29-31], simulation and mechanical modeling [32-35], as well as comparisons to multi-jet fusion (MJF) technology [36-38]. Here, it is worth noting that the literature references related to AM compound materials based on laser-sintered PA12 were not mentioned above, as they are beyond the scope of this study.

In contrast, quite a bit of research has been focused on the mechanical properties of FFF printouts. Gao et al. [39] found that PA12 filaments can accommodate the FFF process under suitable printing parameters, so their quality and mechanical properties highly depend on nozzle and bed temperatures. Li et al. [40] showed that FFF allows the production of PA12 parts with adequate mechanical performance, overcoming the greatest limitation of dependence on amorphous thermoplastics as a feedstock for producing prototypes. Using the Taguchi method, Kam et al. [41] investigated the effects of FFF process parameters on mechanical properties (tensile strength, elongation, and impact strength) of 3D printed PA12 samples. As a result, the layer thickness was found to be the most influential factor for enhancing the mechanical properties instead of extruder temperature, occupancy rate, and filling structure. They also concluded that FFF PA12 could be effectively used to produce many machine parts and mechanical components due to its tensile strength, impact strength resistance, and damping properties. Knoop and Schoeppner [42] conducted their research on FFF Nylon 12 from Stratasys Inc. As this polymer can be processed with three different tip sizes resulting in different layer thicknesses from 178 µm to 330 µm, the corresponding mechanical properties were determined for different build orientations on the printing platform. Vidakis et al. [43] investigated the recycled PA12 filament through extrusion melting over multiple recycling courses, giving insight into its effect on the mechanical and thermal properties of FFF-manufactured specimens obtained throughout the recycling courses. FFF printed specimens were produced from a virgin and recycled PA12 filament, while they have been experimentally tested further for their tensile, flexural, impact, and micro-hardness mechanical properties. It was concluded that PA12 could be a viable option for circular use and 3D printing, offering an overall positive impact on recycling while realizing 3D printed components using recycled filaments with enhanced mechanical and thermal stability. Nonetheless, to the authors' knowledge, no studies have been conducted to compare the flexural properties of Nylon 12 obtained by Fused Filament Fabrication (FFF) versus Selective Laser Sintering (SLS) for different build orientations.

The relevance of the results of this paper can serve as a recommendation when Nylon 12 parts made of FFF or SLS with different print orientations undergoing bending loads are designed to be produced through additive manufacturing. This becomes especially valuable when it comes to selecting which printing technology to use depending on the functionality of printouts and the application requirements.

2. Material and methods

2.1. Specimens

Concerning the additive manufacturing of three-point bending specimens, a Nylon 12 commercially available filament (from Fiberlab S.A.) was selected to employ the fused filament fabrication method (FFF) with a Prusa 3D desktop printer, whereas Nylon 12 sintering powder (from Formlabs Inc.) was chosen for selective laser sintering (SLS) using a benchtop industrial SLS platform, Formlabs Fuse 1, with a powder refresh ratio of 30%.

In preparation for fused filament fabrication (FFF), the specific printing and bed temperatures, layer height, and print speed were selected based on pre-tests that revealed the best qualities of printouts. The employed Nylon 12 filament and 3D printer model and the characteristic printing parameters are reported below.

TABLE 1

The filament material and characteristic printing parameters

Filament specifications	Fiberlogy Nylon PA12 natural, Fiberlab S.A. [44]
Filament diameter	1.75 mm
Printer brand and model	Prusa i3 MK3S
Printing Temperature	250°C
Bed Temperature	70°C
Layer thickness	0.2 mm
Print speed	80 mm/s
Infill density	100%

As a means of the SLS process, the main printing parameters, such as the layer thickness (0.1 mm), the scanning speed (2000 mm/s), and the laser power magnitude (5 W), remained unchanged during the additively manufacturing procedure, while the internal temperature varied during processing between 178.3°C and 178.6°C. A powder refresh ratio of 30% was considered, as Formlabs recommends an interval of 30% to 50% for the ratio of fresh to used powders [45].

The geometric dimensions of three-point bending specimens having 10 mm in width, 80 mm in length, and 4 mm thickness were established according to ISO 178:2019 standard [46]. As shown in Fig. 1, three orientations (i.e., 0°, 45, and 90°) were considered for each type of printing technology (i.e., FFF and SLS).

2.2. Testing

The three-point bending tests were performed at room temperature using a closed-loop Multipurpose Servohydraulic Universal Testing Machine, type LVF 50-HM (Walter-Bai A.G.), as illustrated in Fig. 2-a.

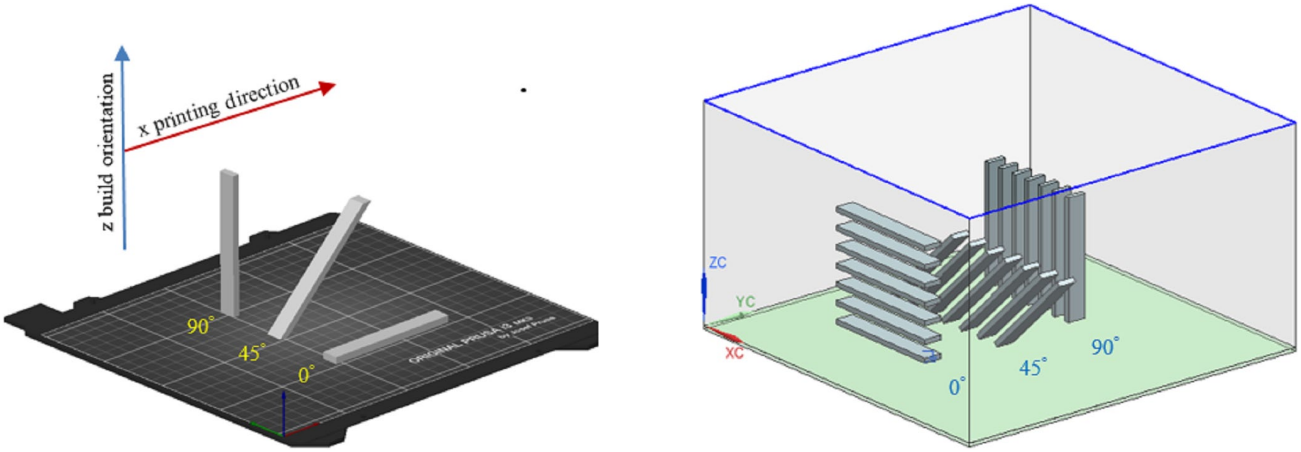

a) Open FFF printing platform

b) SLS orthogonal build space

Fig. 1. The investigated build orientations

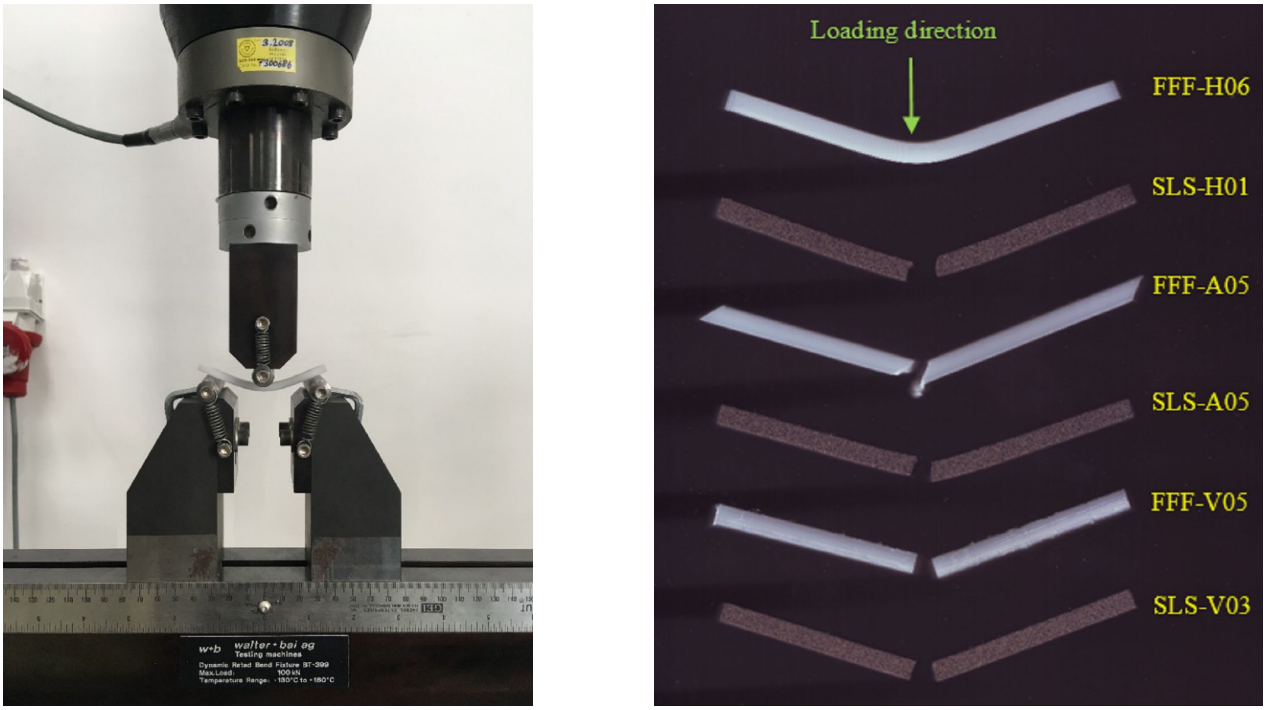

a) FFF specimen undergoing bending test

b) Post-testing FFF and SLS specimens

Fig. 2. Three-point bending test set-up and specimens

The tests were conducted under displacement control with a 1 mm/min crosshead speed. The bending modulus was evaluated between two deflection levels as indicated by ISO 178: 2019 [46]:

$$E_b = \frac{3L^3}{12bh^3} \cdot \frac{F_{0.25\%} - F_{0.05\%}}{s_{0.25\%} - s_{0.05\%}} = \frac{3L^3}{12bh^3} \cdot \frac{\Delta F}{\Delta s} \tag{1}$$

where the values of forces denoted by $F_{0.25\%}$ and $F_{0.05\%}$ together with the associated deflections $s_{0.25\%}$ and $s_{0.05\%}$ correspond to the imposed strains of 0.0025 and 0.0005. The length L indicates the distance between the cylindrical supports in millimeters (mm), b and h are the width and thickness of the specimen in millimeters (mm). A general view of the post-testing specimens' appearance is presented in Fig. 2-b. The label codes are detailed at the beginning of the next section.

A total of 42 specimens were manufactured to perform the bending tests, from which a batch of 21 items was produced by fused filament fabrication technology (SLS), and the second batch of 21 items was obtained through the laser-sintered process (SLS). One-third of each printing batch was printed horizontally, whereas another one-third was built at 45° relative to the printing platform, and the last-third of specimens were built along the vertical direction. All specimens were tested in the as-printed condition, and no subsequent post-processing was applied.

3. Results and discussion

Comparative plots of load-deflection curves between FFF and SLS specimens obtained for the three build orientations under study are represented in Fig. 3, Fig. 4, and Fig. 5. The first group of three letters in the label code refers to the printing technology (SLS or FFF), while the second group returns the specimen build orientation (*H* = horizontal, *A* = angled, *V* = vertical), along with the specimen number identified by the last two digits. For clarity of comparisons, only three representative curves for each pair of printing technology and build orientation are plotted.

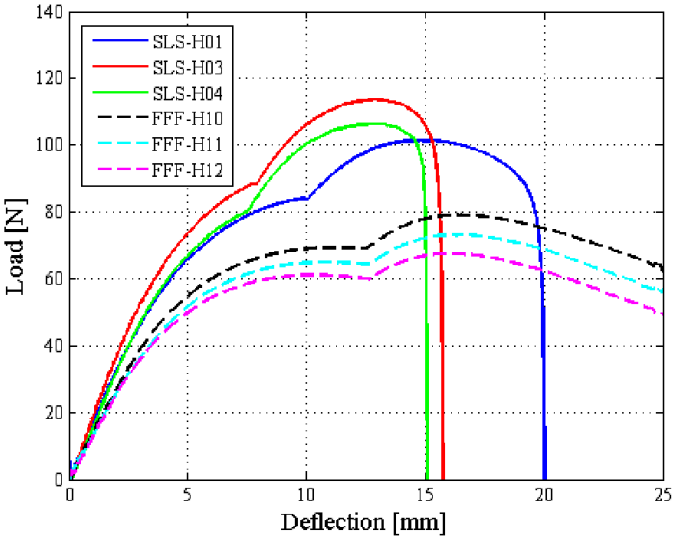

Fig. 3. Load-deflection curves of horizontally printed FFF and SLS specimens

The above figure shows the higher ductility of FFF specimens printed horizontally relative to SLS specimens. Here it is worth mentioning that, for the formers, the tests were stopped when the deflection exceeded 25 mm, while for the laters, an average of 17 mm deflection at break was recorded (see also Fig. 2-b). For both groups of specimens (i.e., SLS and FDM), the applied loads are linearly proportional to the deflection only in the initial loading stage, and the applied loads reach their maximum in a plateau region due to excessive plasticity. Then, the plateau finishes at a knee point that identifies the onset of the specimen shifting upon the cylindrical supports of the three-point bending fixture. Next to the specified knee point, the load-deflection curves exhibit another increasing trend followed by a leveling off and a final decrease, indicating a new level of plasticity during the specimen shifting regime.

A completely different response was exhibited by the specimens printed with 45° and 90° built orientations (see Fig. 4 and Fig. 5). Thus, a load-softening behavior is observed with a primarily nonlinear elastic ascending branch up to the first flexural cracking load. Then, a sudden load drop occurs, followed by an ascending post-elastic region with a maximum load higher than the first critical one. Subsequently, it decreases quite rapidly until the final bending fracture.

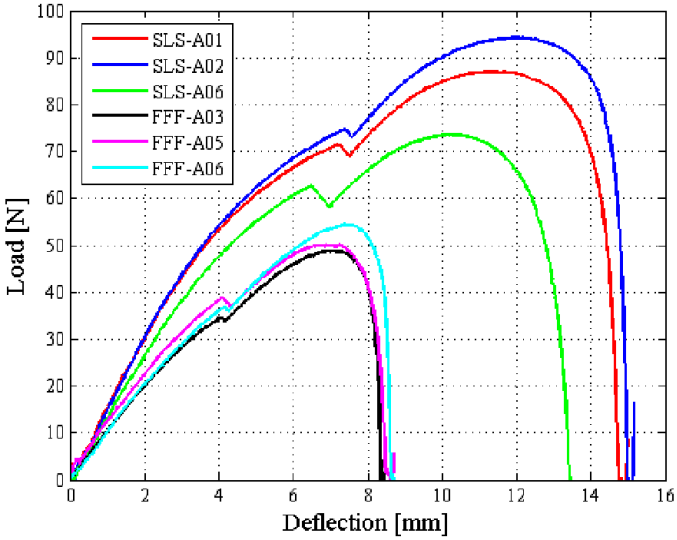

Fig. 4. Load-deflection curves of 45-degree inclined FFF and SLS specimens

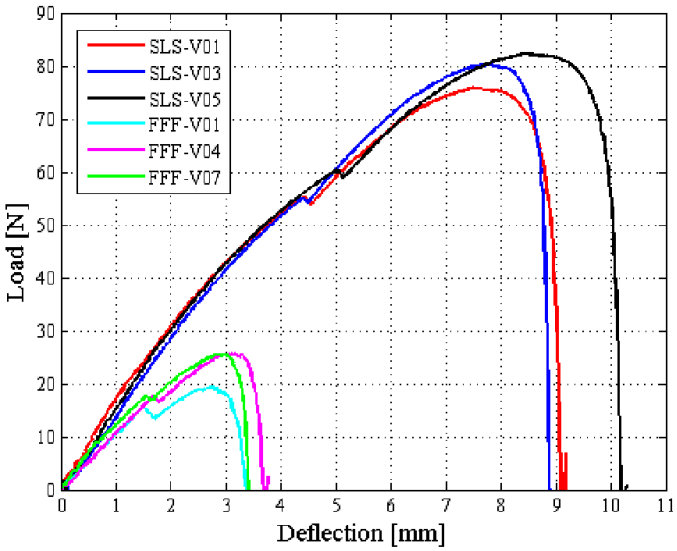

Fig. 5. Load deflection curves of vertically printed FFF and SLS specimens

TABLE 2 reports the basic descriptive statistical parameters related to bending strength and modulus of elasticity in flexure for the three particular build orientations of Nylon 12 produced by FFF and SLS, calculated with the help of IBM SPSS software.

The values of Kolmogorov-Smirnov and Shapiro-Wilk statistics, along with their related significance levels (p), were determined to establish the compliance of test results with a normal distribution and to identify the extreme outliners. The following statistical assumptions were considered: the level of significance ($\alpha = 0.05$), the null hypothesis H0: i.e., the population of the dependent variable from which the samples were extracted follows a normal distribution (for $p > \alpha$), and the alternative hypothesis Ha: i.e., the population from which the sample was extracted does not follow a normal distribution (for $p < \alpha$). TABLE 2 summarizes the results of the normality check performed in IBM SPSS. One can be observed that both the Kolmogorov-Smirnov

TABLE 2

Mean values and standard deviation of bending strength and flexural modulus for three built orientations of Nylon 12 produced by FFF and SLS

Build Orientation (deg.)	Basic statistics		Fused filament fabrication (FFF)		Selective laser sintering (SLS)	
			Bending strength (MPa)	Flexural modulus (MPa)	Bending strength (MPa)	Flexural modulus (MPa)
0°	Mean value		57.9	1464.7	81.1	1892.8
	Std. Deviation		5.86	107.22	6.89	51.88
	95% Confidence Interval for Mean	Lower Bound	53.72	1387.98	74.72	1838.33
		Upper Bound	62.11	1541.39	87.47	1947.23
45°	Mean value		34.5	1133.9	69.7	1689.5
	Std. Deviation		3.15	130.76	5.47	87.38
	95% Confidence Interval for Mean	Lower Bound	31.21	996.70	64.64	1768.76
		Upper Bound	37.82	1271.15	74.76	1990.14
90°	Mean value		16.9	1257.2	59.6	1879.4
	Std. Deviation		3.57	289.52	4.2	105.47
	95% Confidence Interval for Mean	Lower Bound	14.01	1015.18	55.74	1648.27
		Upper Bound	19.98	1499.28	63.55	1990.97

TABLE 3

Results of Kolmogorov-Smirnov and Shapiro-Wilk tests for bending strength normality check

Print technology	Build orientation (deg.)	Kolmogorov-Smirnov**			Shapiro-Wilk		
		Statistic	df	Sig.	Statistic	df	Sig.
FDM	0°	0.149	10	0.200*	0.972	10	0.908
	45°	0.171	6	0.200*	0.983	6	0.966
	90°	0.175	8	0.200*	0.954	8	0.755
SLS	0°	0.193	7	0.200*	0.941	7	0.647
	45°	0.154	7	0.200*	0.967	7	0.879
	90°	0.183	7	0.200*	0.892	7	0.283

* This is a lower bound of the true significance
** Lilliefors Significance Correction

and Shapiro-Wilk test data suggest that bending strength and flexural modulus follow a normal distribution.

In the next stage, a one-way analysis of variance (ANOVA) was carried out to assess the statistical variability of experimental data and compare the mean values of bending strength and flexural moduli for the three build orientations of Nylon 12 manufactured through FFF and SLS. In particular, Levene's test was utilized to analyze the homogeneity of variance within the six analyzed groups (their identification labels are shown in Fig. 4, Fig. 5, and Fig. 6) for each dependent variable (i.e., bending strength and flexural modulus). The null hypothesis H0 assumes that the variances in the six analyzed groups are homogeneous ($p > \alpha = 0.05$), while they are heterogeneous for the alternative hypothesis Ha, ($p < \alpha = 0.05$). As reported in TABLE 5, the results related to the bending strength variable indicate homogeneous variances over all the analyzed groups,

TABLE 4

Results of Kolmogorov-Smirnov and Shapiro-Wilk tests for flexural modulus normality check

Print technology	Build orientation (deg.)	Kolmogorov-Smirnov**			Shapiro-Wilk		
		Statistic	df	Sig.	Statistic	df	Sig.
FDM	0°	0.212	10	0.200*	0.972	10	0.199
	45°	0.189	6	0.200*	0.983	6	0.694
	90°	0.194	8	0.200*	0.954	8	0.378
SLS	0°	0.228	6***	0.200*	0.859	6***	0.185
	45°	0.210	7	0.200*	0.967	7	0.115
	90°	0.176	6***	0.200*	0.926	6***	0.547

* This is a lower bound of the true significance.
** Lilliefors Significance Correction
*** Recalculated values after removing one outliner

TABLE 5

Results for homogeneity of variances tests

The Independent variable	Test criteria	Levene Statistic	df1	df2	Sig.
Bending strength	Based on Mean	1.588	5	39	0.186
	Based on Median	1.090	5	39	0.381
	Based on Median and with adjusted df	1.090	5	30.256	0.386
	Based on trimmed mean	1.581	5	39	0.188
Flexural modulus	Based on Mean	4.401	5	37	0.003
	Based on Median	3.954	5	37	0.006
	Based on Median and with adjusted df	3.954	5	16.012	0.016
	Based on trimmed mean	4.350	5	37	0.003

with the minimum significance level, $p = 0.186 > \alpha = 0.05$ (based on the mean value), whereas the data calculated for the modulus of elasticity in flexure return the heterogeneity of variances, with a minimum significance level ($p = 0.003 < \alpha = 0.05$) between the six groups (based on the mean and trimmed mean values). In addition, the ANOVA test results show that the level of probability between all analyzed groups of specimens for both dependent variables ($p < \alpha = 0.05$) rejects the null hypothesis and supports the alternative one (i.e., at least two mean values differ from each other).

Although the ANOVA test shows the overall significance of three-point bending test results, it does not specify where the actual differences lie. Thus, after running the ANOVA one-way analysis, Tukey's HSD and Games-Howell tests have been considered to evaluate which mean values of the six analyzed groups (relative to each other) are different as it compares all possible pairs of mean values. Reasonable differences between bending strength and flexural elasticity modulus were obtained for the assumed significance *p*-level of 0.05.

Fig. 6 shows the comparative plots of bending strength and flexural modulus mean values and standard deviations for the three analyzed build orientations (i.e., 0°, 45°, and 90°) and two printing technologies (i.e., FFF versus SLS). Regarding the bending strength, the mean value obtained for SLS horizontally built specimens is 28% higher than that of FFF specimens with the same orientation. A slight decrease in bending strength can be observed with the increase of building orientation angle for SLS specimens, while the decrease is more significant for FFF specimens. However, the values of bending strength obtained for SLS are of the same magnitude order as the ones reported in the literature [21,26,31].

Regarding the flexural modulus, its mean value for SLS horizontally built specimens is 23% higher than that obtained for FFF specimens with the same built orientation. Nevertheless, the flexural modulus of the SLS specimens printed in 45° orientation was 32% higher than that of FFF printed counterparts. Small differences can be observed between the flexural modulus of horizontally and vertically oriented specimens processed either with SLS or FFF techniques. Moreover, in terms of flexural elasticity modulus, both FFF and SLS vertically built specimens performed better than specimens built at 45° orientation.

4. Conclusions

This study compared the three-point bending response of Nylon 12 printed by FFF versus SLS, i.e., a filament-based 3D printing technique and a powder bed fusion printing process. Specimens have been manufactured in three different build orientations relative to the printing platform (i.e., 0°, 45°, and 90°). The conclusions can be drawn as follows:

The general trend of load-deflection curves relative to the build orientation differs from the actual tensile stress-strain curves reported in the literature. This observation confirms the thesis of an accentuated anisotropy in bending compared to the tensile loading.

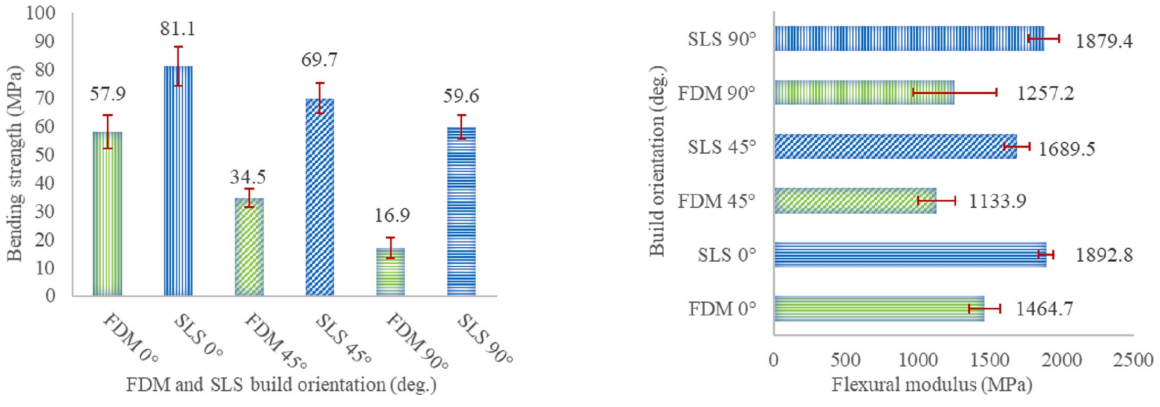

a) Bending strength

b) Flexural modulus

Fig. 6. Comparative plots of bending strength and flexural modulus for the three different build orientations and printing technologies

As the bending strength decreases slightly with the increase of building orientation angle for SLS specimens, while for FFF specimens, the decrease is more apparent, a significant build orientation-dependent anisotropy in bending strength of FFF specimens compared to SLS was discovered. The mean value of bending strength obtained for SLS horizontally built specimens is 28% higher than FFF specimens with the same orientation. However, the FFF specimens printed horizontally exhibit a higher ductility relative to SLS specimens.

Regarding the flexural modulus, its mean value for SLS horizontally built specimens was found to be 23% higher than the one obtained for FFF specimens with the same built orientation. Nevertheless, the flexural modulus of the SLS specimens printed in 45° orientation was 32% higher than that of FFF printed counterparts. Small differences can be observed between the flexural modulus of horizontally and vertically printed specimens either for SLS or FFF. A surprising result of this investigation is that the specimens built with 90° orientation showed superior modulus elasticity in flexure but a low bending strength compared to 45° oriented specimens.

Homogeneity of variances was obtained for bending strength between all the analyzed groups of specimens with different build orientations and printing technologies, whereas the mean values of flexural modulus do not.

REFERENCES

[1] M. Sperry, A. Busath, M. Ottesen, J. Heslington, N. Crane, Post-Processing and Material Properties of Nylon 12 Prepared by Laser-Powder Bed Fusion, ASME International Mechanical Engineering Congress and Exposition. American Society of Mechanical Engineers **85567**, V02BT02A031 (2021).

[2] J. Rydz, W. Sikorska, M. Kyulavska, D. Christova, Polyester-based (bio) degradable polymers as environmentally friendly materials for sustainable development, International Journal of Molecular Sciences **16** (1), 564-596 (2014).

[3] A. Awad, F. Fina, A. Goyanes, S. Gaisford, A.W. Basit, 3D printing: Principles and pharmaceutical applications of selective laser sintering, International Journal of Pharmaceutics **586**, 119594 (2020).

[4] D.W. Martinez, M.T. Espino, H.M. Cascolan, J.L. Crisostomo, J.R.C. Dizon, A Comprehensive Review on the Application of 3D Printing in the Aerospace Industry, Key Engineering Materials **913**, 27-34 (2022).

[5] S. Saleh Alghamdi, S. John, N. Roy Choudhury, N.K. Dutta, Additive manufacturing of polymer materials: Progress, promise and challenges. Polymers **13** (5), 753 (2021).

[6] S. Singh, A. Sachdeva, V.S. Sharma. A study on selective laser sintered parts for dimensional and surface characteristics, Journal of Manufacturing Technology Research, **4** (3-4), 145-157 (2012).

[7] S. Dupin, O. Lame, C. Barrès, J.Y. Charmeau, Microstructural origin of physical and mechanical properties of polyamide 12 processed by laser sintering, European Polymer Journal **48** (9), 1611-1621 (2012).

[8] J.P. Kruth, P. Mercelis, J. Van Vaerenbergh, L. Froyen, M. Rombouts, Binding mechanisms in selective laser sintering and selective laser melting. Rapid Prototyping Journal **11** (1), 26-36 (2005).

[9] R.D. Goodridge, C.J. Tuck, R.J.M. Hague, Laser sintering of polyamides and other polymers, Progress in Materials Science **57** (2), 229-267 (2012).

[10] B.N. Turner, R. Strong, S.A. Gold, A review of melt extrusion additive manufacturing processes: I. Process design and modeling, Rapid Prototyping Journal **20** (3), 192-204 (2014).

[11] J. Kotlinski, Mechanical properties of commercial rapid prototyping materials, Rapid Prototyping Journal **20** (6), 499-510 (2014).

[12] A. Kafle, E. Luis, R. Silwal, H.M. Pan, P.L. Shrestha, A.K. Bastola, 3D/4D Printing of polymers: Fused deposition modelling (FDM), selective laser sintering (SLS), and stereolithography (SLA), Polymers **13** (18), 3101 (2021).

[13] L. Feng, Y. Wang, Q. Wei, PA12 Powder Recycled from SLS for FDM, Polymers **11** (4), 727 (2019).

[14] D.G. Zisopol, I. Nae, A.I. Portoaca, I. Ramadan, A Statistical Approach of the Flexural Strength of PLA and ABS 3D Printed Parts, Engineering, Technology & Applied Science Research **12** (2), 8248-8252 (2022).

[15] P.K. Jain, P.M. Pandey, P.V.M. Rao, Experimental investigations for improving part strength in selective laser sintering, Virtual and Physical Prototyping **3** (3), 177-188 (2008).

[16] T.L. Starr, T.J. Gornet, J.S. Usher, The effect of process conditions on mechanical properties of laser-sintered nylon, Rapid Prototyping Journal **17** (6), 418-423 (2011).

[17] E.C. Hofland, I. Baran, D.A. Wismeijer, Correlation of process parameters with mechanical properties of laser sintered PA12 parts, Advances in materials science and engineering **4953173**, 11 (2017).

[18] A. Pilipović, T. Brajlih, I. Drstvenšek, Influence of processing parameters on tensile properties of SLS polymer product, Polymers **10** (11), 1208 (2018).

[19] L.L. Dincă, N.M. Popa, N.L. Milodin, C. Stanca, D. Gheorghiu, Influence of the process parameters on mechanical properties of the final parts obtained by selective laser sintering from PA2200 powder, MATEC Web Conf. **299**, 11 (2019).

[20] F. Lupone, E. Padovano, F. Casamento, C. Badini, Process Phenomena and Material Properties in Selective Laser Sintering of Polymers: A Review, Materials **15** (1), 183 (2021).

[21] U. Ajoku, N. Saleh, N. Hopkinson, R. Hague, P. Erasenthiran, Investigating mechanical anisotropy and end-of-vector effect in laser-sintered nylon parts, Proceedings of the Institution of Mechanical Engineers, Part B: Journal of Engineering Manufacture **220** (7), 1077-1086 (2006).

[22] B. Caulfield, P.E. McHugh, S. Lohfeld, Dependence of mechanical properties of polyamide components on build parameters in the SLS process, Journal of Materials Processing Technology **182** (1-3), 477-488 (2007).

[23] C. Majewski, N. Hopkinson, Effect of section thickness and build orientation on tensile properties and material characteristics of laser sintered nylon-12 parts, Rapid Prototyping Journal **17** (3), 176-180 (2011).

[24] W. Cooke, R.A. Tomlinson, R. Burguete, D. Johns, G. Vanard, Anisotropy, homogeneity and ageing in an SLS polymer, Rapid Prototyping Journal **17** (4), 267-279 (2011).

[25] L. Marsavina, D.I. Stoia, Flexural properties of selectively sintered polyamide and Alumide, Material Design & Processing Communications **2** (1), e112 (2012).

[26] C.S. Miron-Borzan, M.C. Dudescu, P. Berce, Bending and compression tests for PA 2200 parts obtained using Selective Laser Sintering method, MATEC Web Conf. **94**, 03010 (2017).

[27] M. Tomanik, M. Żmudzińska, M. Wojtków, Mechanical and Structural Evaluation of the PA12 Desktop Selective Laser Sintering Printed Parts Regarding Printing Strategy, 3D Printing and Additive Manufacturing **8** (4), 271-279 (2021).

[28] M.N. Baba, Flatwise to Upright Build Orientations under Three-Point Bending Test of Nylon 12 (PA12) Additively Manufactured by SLS, Polymers **14** (5), 1026 (2022).

[29] S. Singh, V.S. Sharma, A. Sachdeva, S.K. Sinha, Optimization and analysis of mechanical properties for selective laser sintered polyamide parts, Materials and Manufacturing Processes **28** (2), 163-172 (2013).

[30] J. Wu, X. Xu, Z. Zhao, M. Wang, J. Zhang, Study in performance and morphology of polyamide 12 produced by selective laser sintering technology, Rapid Prototyping Journal **24** (5), 813-820 (2018).

[31] J. Schneider, S. Kumar, Multiscale characterization and constitutive parameters identification of polyamide (PA12) processed via selective laser sintering, Polymer Testing **86**, 106357 (2020).

[32] D.A. Şerban, G. Weber, L. Marşavina, V.V. Silberschmidt, W. Hufenbach, Tensile properties of semi-crystalline thermoplastic polymers: Effects of temperature and strain rates, Polymer Testing **32** (2), 413-425 (2013).

[33] P. Obst, M. Launhardt, D. Drummer, P.V. Osswald, T.A. Osswald, Failure criterion for PA12 SLS additive manufactured parts, Additive Manufacturing **21**, 619-627 (2018).

[34] F.R.Phillips, T.C. Henry, J. Hrynuk, R.A. Haynes, E. Bain, J. Westrich, Utilization of Three-Point Bending for Numerical Prediction of Structural Response in Additively Manufactured Parts, US Army Combat Capabilities Development Command Army Research Laboratory Austin United States. (2020).

[35] R. Brighenti, M.P. Cosma, L. Marsavina, A. Spagnoli, M. Terzano, Laser-based additively manufactured polymers: A review on processes and mechanical models, Journal of Materials Science **56** (2), 961-998 (2021).

[36] S. Rosso, R. Meneghello, L. Biasetto, L. Grigolato, G. Concheri, G. Savio, In-depth comparison of polyamide 12 parts manufactured by Multi Jet Fusion and Selective Laser Sintering, Additive Manufacturing **36**, 101713 (2020).

[37] C. Cai, W.S. Tey, J. Chen, W. Zhu, X. Liu, T. Liu, L. Zhao, K. Zhou, Comparative study on 3D printing of polyamide 12 by selective laser sintering and multi jet fusion, Journal of Materials Processing Technology **288**, 116882 (2021).

[38] F. Calignano, F. Giuffrida, M. Galati, Effect of the build orientation on the mechanical performance of polymeric parts produced by multi-jet fusion and selective laser sintering, Journal of Manufacturing Processes **65**, 271-282 (2021).

[39] X. Gao, D. Zhang, X. Wen, S. Qi, Y. Su, X. Dong, Fused deposition modeling with polyamide 1012, Rapid Prototyping Journal **25** (7), 1145-1154 (2019).

[40] H. Li, S. Zhang, Z. Yi, J. Li, A. Sun, J. Guo, G. Xu, Bonding quality and fracture analysis of polyamide 12 parts fabricated by fused deposition modeling, Rapid Prototyping Journal **23** (6), 973-982 (2017).

[41] M. Kam, A. Ipekçi, Ö. Sengül, Investigation of the effect of FDM process parameters on mechanical properties of 3D printed PA12 samples using Taguchi method, J. Thermoplast. Compos. Mater. **08927057211006459**, 1-5 (2021).

[42] F. Knoop, V. Schoeppner, Mechanical and thermal properties of FDM parts manufactured with polyamide 12, Proceedings of the 26th Annual International Solid Freeform Fabrication Symposium – An Additive Manufacturing Conference, Austin, TX, USA, 10-12 (2015).

[43] N. Vidakis, M. Petousis, L. Tzounis, A. Maniadi, E. Velidakis, N. Mountakis, J.D. Kechagias, Sustainable additive manufacturing: Mechanical response of polyamide 12 over multiple recycling processes, Materials **14** (2), 466 (2021).

[44] https://c-3d.niceshops.com/upload/file/FIBERLOGY_NYLON_PA12_TDS.pdf (Accessed 31 March 2022).

[45] https://formlabs-media.formlabs.com/datasheets/2001447-TDS-ENUS-0.pdf (Accessed 31 March 2022).

[46] ISO 178: 2019, Plastics – determination of flexural properties, ISO Committee, Geneva, (2019).